Batteries & Supercaps

Research Article
doi.org/10.1002/batt.202500610

Chemistry Europe
European Chemical Societies Publishing

www.batteries-supercaps.org

Investigation of Degradation Pathways in Fluoroethylene Carbonate Based Electrolytes via Chromatographic Techniques

Nick Fehlings, Matthias Weiling, Jakob Hesper, Maximilian Kubot, Martin Winter, Simon Wiemers-Meyer, and Sascha Nowak*

For enhancing battery key performance indicators, like high voltage, safety, or lifetime, tailored electrolytes are crucial. Additives enable modifications of the solid electrolyte interphase (SEI) improving its electrochemical stability or mechanical strength. The formation and composition of the SEI still require further optimization. During operation, various side reactions of the electrolyte occur, resulting in continuous consumption of active material. The clarification of degradation mechanisms helps in understanding aging phenomena emerging during cycling. This article investigates different electrolytes formulations containing varying amounts fluoroethylene carbonate (FEC) for employment in high voltage applications. Long-term cycling revealed roll over effect occurring for the use of FEC and EC as cosolvents and highest capacity retention for FEC replacing EC. Subsequent *post mortem* electrolyte analysis by means of high-performance liquid chromatography coupled to quadrupole time of flight analyzer revealed the formation of FEC related degradation products. FEC undergoes subtraction of fluoride to form in situ VC which then continuously reacts with other electrolyte components. The identification of degradation products thus provides information about the degradation processes, confirmed for the first time by means of instrumental analytics.

1. Introduction

The increasing global demand for high energy has driven the development of state-of-the-art (SOTA) lithium ion batteries (LIB).[1] Especially in aspect of climate change, the electric mobility is an increasing application field for LIBs in order to reduce CO_2 emissions.[2,3] LIBs are continuously improved to achieve higher energy density, long-term stability, and lower production costs.[4] These targets can be realized by tailoring electrolyte, active materials as well as cell design.[5,6]

Most SOTA LIBs consist of a layered lithium metal oxides (e.g. $LiNi_xMn_yCo_zO_2$) or lithium iron phosphate ($LiFePO_4$), a carbonaceous negative electrode and a separator which is soaked with the electrolyte.[7,8] Employed electrolytes consist of different solvents, mostly linear (e.g. ethyl methyl carbonate (EMC), dimethyl carbonate (DMC)) and cyclic carbonates (e.g. ethylene carbonate (EC), propylene carbonate (PC)), a conducting salt (e.g. $LiPF_6$), and additives (e.g. vinylene carbonate (VC), fluoroethylene carbonate (FEC)).[9] Combination of those components not only enables high ionic conductivity but also offer stability over wide voltage windows.

During cell formation, electrolyte components such as EC or additives are being reductively decomposed at the surface of the negative electrode forming the solid electrolyte interphase (SEI).[10] The SEI consists of organic and inorganic parts which are in the ideal case electronically insulating but permeable for lithium ions ensuring the ionic conductivity and at the same time hindering continuously further degradation during cycling. However, during formation, electrolyte consumption and lithium loss are observed, resulting in around 10%–20% capacity loss.[11] Despite numerous advantages, the SEI still faces challenges which needs to be improved. Structural changes during charge of the negative electrode influence the morphology of the SEI.[12] Thus, cracking of the SEI can occur revealing fresh electrode surface which is then exposed to electrolyte. The electrolyte and lithium ions then continuously degrade on the fresh electrode surface, further reducing the overall capacity.[12] The progressive electrolyte degradation can ultimately result in drying of the cell preventing ongoing cycling.[13] Continuous drying of the electrolytes leads to immobilization of the electrode and insufficient lithium transport which increases cell resistance and further reduces battery performance.[14] Additionally, the SEI can thicken by further electrolyte decomposition, resulting in increased resistance and poorer electrochemical properties.[15] The formulation of the electrolyte, by tailoring it with additives, influences structural stability and properties of the SEI.[16]

Film forming additives, such as VC and FEC, help prevent further electrolyte degradation. During formation, the additives are consumed before EC and get incorporated into the SEI, altering

N. Fehlings, J. Hesper, M. Kubot, M. Winter, S. Wiemers-Meyer, S. Nowak
University of Münster
MEET Battery Research Center
Corrensstraße 46, 48149 Münster, Germany
E-mail: sascha.nowak@uni-muenster.de

M. Weiling, M. Winter
Helmholtz-Institute Münster
IMD-4 FZ Jülich
Corrensstraße 46, 48149 Münster, Germany

its composition by accumulating additive based components.[17] For FEC, literature showed that the SEI exhibits increased flexibility and increased LiF content.[18] Modified SEIs are suitable for high-voltage applications due to their increased electrochemical, attributable to increased fluoride content, stability window, and mechanical strengths.[19] High voltage application complicates the utilization of standard electrolytes as more reactive species are being formed.[20] Due to decomposition of EC at voltages of <0.8 V versus Li^+/Li,[21] additives or cosolvents, especially FEC, are widely investigated.[22] The decomposition of EC already occurs for cell voltages above 4.4 V, which would disable upper cut-off voltages application as the decomposition result in severe gassing and aging of the electrolyte.[23,24] Despite electrochemical improvements with FEC electrolytes, the aging mechanism is still not fully understood. Different studies by Kim et al. suggest the formation of polyethylene glycol co-oligomers with possibilities of fluoride entities.[25] Other studies described that FEC reacts via fluoride subtraction to in situ formed VC which then further behaves similarly to VC by being polymerized and incorporated into the SEI.[26,27] However, all FEC degradation mechanisms proposed guarantee comprehensive improvement in electrochemical performance. New studies investigating FEC substitution of EC have shown that the improved cycling behavior can be attributed to decreased electrolyte degradation, transition metal dissolution, and better SEI formation.[28,29] Terreblanche et al. showed that EC and FEC as cosolvents showed inferior electrochemical stability compared with its EC-free counterpart.[29] However, to continuously improve the electrolyte in regard of ensuring better SEI formation and decreased electrolyte degradation, it is crucial to understand the underlying aging mechanisms.[19]

Therefore, several analytical methodologies are reported to elucidate the aging phenomena emerging during cycling.[30,31] For electrolyte aging, various separation techniques, like liquid, gas, or ionic chromatography, are described.[32–34] Studies by Henschel et al. showed promising capabilities verifying degradation mechanisms for different electrochemical operations or standard electrolyte formulations.[35,36] Thus, analysis of degradation products enables deeper insights into the exact mechanism occurring. During cell operation, the continuous degradation results in increased molecular weight of decomposition products, which outranges of the solvents and may hinder the application of gas chromatography (GC). High-performance liquid chromatography (HPLC) with a high-resolution mass analyzer (MS) and MS^2 fragmentation capabilities provide accurate identification of formed decomposition products.[37]

In this work, the influence of FEC concentrations in the electrolyte was investigated with an established method of HPLC hyphenated to quadrupole time of flight analyzer (QToF). Long-term cycling was performed to determine the influence on formed degradation products. Additionally, two upper cut-off voltages were investigated as various amounts of degradation reactions occur for high voltage applications. Ultimately, the FEC degradation mechanism on the long postulated in situ VC formation[26] was approved by identifying degradation products originating from FEC. Thus, conclusions about the SEI composition can be obtained as VC polymers tend to polymerize and precipitate on the negative electrode.[38]

2. Experimental Section

2.1. Chemicals and Materials

Ethyl methyl carbonate (EMC; 99.9%), ethylene carbonate (EC; 99.9%), and fluoroethylene carbonate (FEC; 99.9%) were purchased from Solvionic (Toulouse, France). $LiPF_6$ (99.89%) was obtained from BASF (Ludwigshafen, Germany). Furthermore, acetonitrile (ACN, hypergrade, Merck KGaA, Darmstadt) and deionized water (Millipore, Molsheim, France; 18.2 MΩ cm^{-1}) were used as eluents and sample dilution. Electrolytes were formulated by an in-house robotic high throughput system in a glove box (O_2, $H_2O < 0.1$ ppm). All chemicals were used as received. All electrolytes contained 1 mol L^{-1} $LiPF_6$, EMC (70 wt. %) and EC or FEC in varying concentrations shown in **Table 1**.

2.2. Cell Assembly and Electrochemical Operation

Commercially available LIB pouch cells (Li-Fun NMC622||graphite, 200 mAh) were dried under reduced pressure for 24 h at 80 °C. The cells were filled with 700 µL of the respective electrolyte formulation (Table 1) and sealed with a relative pressure of −90 kPa for 5 s. After wetting for 20 h, three constant current (CC) charge (0.1 C) and CC discharge (0.1 C) cycles were performed in a voltage window between 4.2 and 3.0 V, and 4.5 and 3.0 V. After formation, long-term cycling was performed for 600 CC (1.0 C) charge and 600 CC (1.0 C) discharge cycles.

2.3. Analytical Measurements

After electrochemical application, all cells were opened in a glovebox (O_2, $H_2O < 0.1$ ppm) and electrolytes were extracted via centrifugation of the electrode-separator stack at 9500 rpm for 20 min. Investigation of thermally and electrochemically induced LIB electrolyte decomposition products were performed with an UltiMate U3000 HPLC (Thermo Fisher Scientific, USA) hyphenated to a 6530 Q-TOF (Agilent). Reversed-phase chromatography was conducted on a ZORBAX SB-C18 column (100 × 2.1 mm, 1.8 µm; Agilent Technologies, Inc., Santa Clara, CA, USA) at 40 °C and a flow rate of 0.5 mL min^{-1}. Sample preparation was conducted according to Henschel et al., while chromatographic separation was adapted.[39] The mobile phase consisted of 0.1 V% formic acid (A) and acetonitrile (B). The gradient started with 5% B from 0 to 1.9 min and increased to 70% B within 12.1 min. Subsequently, the mobile phase was kept constant at 60% B for 6 min.

Table 1. Compositions of all electrolytes investigated via HPLC-QToF.

STD	F1	F1.5	F2	F3
EC:EMC 3:7	EC:FEC:EMC 2:1:7	EC:FEC:EMC 1.5:1.5:7	EC:FEC:EMC 1:2:7	FEC:EMC 3:7

Finally, the column was equilibrated at 5% B for 4 min. The injection volume was 5 μL. To protect the QToF mass spectrometer from high concentrations of conducting salts, the flow line switched to the MS after 1.9 min. Ionization was performed in ESI(+) mode. The source parameters were: gas temperature 350 °C, drying gas flow 10 mL min^{-1}, nebulizer pressure 45 psi, and VCap 3000 V. The mass range was set to a mass-to-charge (*m/z*) of 100–1700 and 90–1000 with an acquisition rate of 4 spectra s^{-1}. The collision-induced energy was set to 10 eV. A mzmine (version: 4.4.3, mzio) was used for HP LC-MS data evaluation.[40] All samples were diluted 1:100 with ACN for measurements.

2.4. Theoretical Calculations

Density functional theory (DFT) calculations were carried out using the Gaussian16 package.[41] All geometries were optimized using B3LYP DFT functional and the 6–311++G(3df, 2p) basis set. The effect of a surrounding electrolyte was mimicked by SMD implicit solvation model using parameters for acetone, showing a similar dielectric constant as liquid carbonate-based electrolytes.[42–46] The electronic energies for the putative reactions were calculated with thermal energy correction (298.15 K).

3. Results and Discussion

Different electrolytes were investigated in commercially available pouch level cells (NMC622||AG) and cycled for 600 cycles (1.0 C). The employment of FEC as cosolvent with concentrations of 10% and 15% (F1 and F1.5) revealed worse long-term stability but higher capacity for 200 cycles than STD (1 M $LiPF_6$, EC:EMC 3:7) at the upper cut-off of 4.5 V, shown in **Figure 1**a. In contrast, STD exhibits the highest initial capacity which can be attributed to improved Li^+ solvation and decreased viscosity of EC-based compared to FEC-based electrolytes. FEC-based electrolytes are more viscous due to stronger intermolecular forces, while the lower viscosity of EC-based electrolytes result in better ionic conductivity.[47,48] Roll over effects for F1, F1.5, and F2 (20% FEC) occur after 200, 250, and 300 cycles respectively. The roll over effect describes the point where linear cell aging transitions to rapid capacity loss. Typically, it is driven by progressive loss of active lithium, transition metal dissolution, thickening of SEI, and/or lithium plating contributing to decrease in capacity. Each following cycle then amplifies previous damage and capacity declines more rapidly. Higher FEC concentrations (20% and 30%; F2 and F3) improve cycle stability. The highest capacity and capacity retention is observed for replacing EC with FEC. Studies by Klein et al. showed beneficial effects for EC-free electrolytes on cycling with higher cut-off voltages.[49] Therefore, FEC as cosolvent with EC employed in high voltage LIBs results in accelerated capacity fading. For upper cut-off voltage 4.2 V (Figure 1b), no roll over effect occurs indicating less degradation of active material as well as the electrolyte. The capacity retention does not improve with higher FEC content in the electrolytes, indicating that the optimum FEC concentration for FEC-EC-based electrolytes is achieved at lower FEC concentrations. However, like the high voltage application, F3 (no EC) has the highest and STD the lowest capacity. Lower cut-off voltages do not result in roll over effect matching literature. Less side reactions occur during cycling, for example, electrolyte degradation or transition metal dissolution, which would decrease cell performance.[50]

HPLC measurements of electrolytes detect degradation products, which are soluble in the electrolyte, thus enabling monitoring the electrolytes state of health.[34] The highest intensities for STD with higher cut-off voltages, depicted in **Figure 2**a, correlate to electrochemical data as more severe capacity loss is observable. All peaks correspond to EC, EMC, or $LiPF_6$ related degradation products previously identified by Jonas Henschel et al.[35,39] Increased intensity of degradation products can be correlated to state of health of the electrolyte. In literature, its stated that high voltage shows increased degradation of electrolytes, thus the electrolyte of 4.5 V STD exhibits severe electrolyte aging compared to 4.2 V STD. Overall, total intensity for FEC-containing electrolytes (Figure 2b) is lower but more distinct peaks are detected. Thus, degradation products of FEC/EC may show an influence on long-term stability of the cell. In regard of FEC, the highest intensity behaves similar to electrochemical performance with F1 showing the highest amounts of peaks. Specific peaks only related to FEC were found for F1–F3 which are elucidated in the following section. With decreased intensity for FEC-containing electrolytes, less

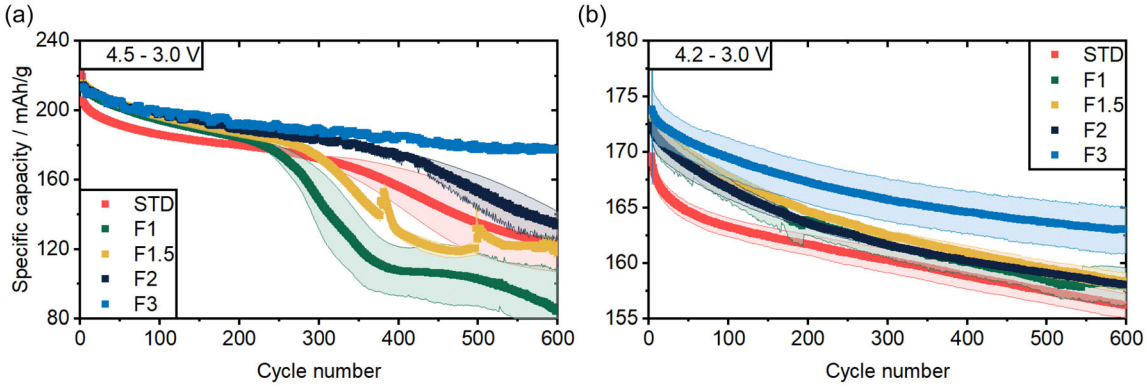

Figure 1. Specific capacity of pouch cells (NMC622||AG, 200 mAh, 1.0 C) for 600 cycles and different cut-off voltages of a) 4.5 V and b) 4.2 V. Different electrolytes with increasing FEC as cosolvent were employed.

Research Article
doi.org/10.1002/batt.202500610
Chemistry Europe
European Chemical Societies Publishing

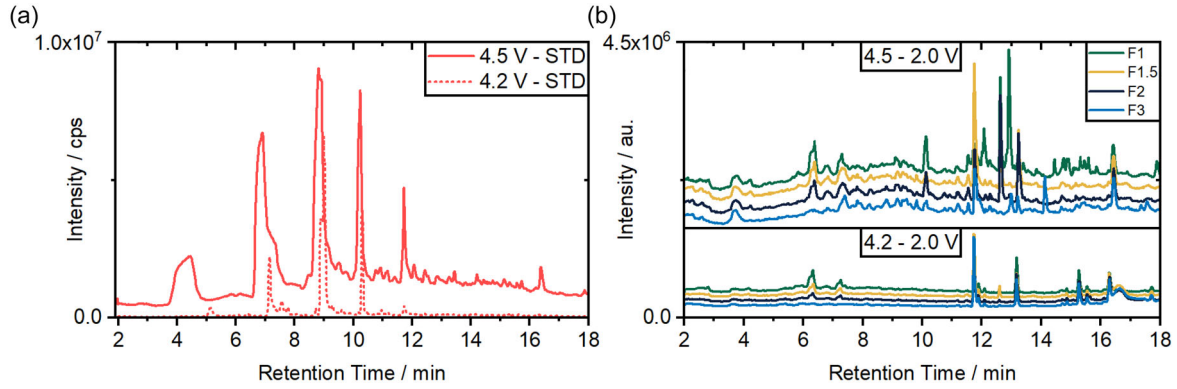

Figure 2. Total ion chromatograms (TICs) measured with HPLC-QToF of investigated electrolytes with an increasing FEC content for 4.5 and 4.2 V upper cut-off voltages. a) shows the TICs of the STD electrolyte while b) shows the TICs for FEC-containing electrolytes. 4.5 V is depicted as line and 4.2 V as points.

electrolyte aging is suspected, but increased amounts of distinct peaks making it difficult to correlate to state of health for the high voltage applications. The low amounts and intensities of peaks for lower cut-off voltage in FEC-containing electrolytes indicate that the state of health of the electrolyte remains stable correlating to electrochemical data.

3.1. Structure Elucidation

Structure elucidation of FEC related degradation products found in Figure 2 was performed by means of HPLC-QToF and fragmentation experiments (**Figure 3**). In Figure 3a, the adduct pattern of the precursor ion with *m/z* 238.0915 $[M+NH_4]^+$ is displayed. The postulated sum formula $C_8H_{13}O_7$ has a relative mass deviation of <5 ppm ($m/z_{calc.} = 238.0921$ $[M+NH_4]^+$) and double bond equivalent (DBE) of 3. MS^2 spectrum shown in Figure 3b indicates the presence of terminal carbonate moiety as both fragment *m/z* 117.0546 $[M+H]^+$ and *m/z* 89.0227 $[M+H]^+$ which correlate to $C_3H_4O_3$ and $C_5H_8O_3$ originate from diethyl carbonate. Fragment *m/z* 133.0492 $[M+H]^+$ and *m/z 149.0417* $[M+H]^+$ both correlate to the loss of terminal carbonate moiety revealing the presence of VC unit in the molecule. Fragment *m/z 89.0227* $[M+H]^+$ corresponds to loss of carbonate and decarboxylation of the precursor molecule further confirming the structural proposal shown in

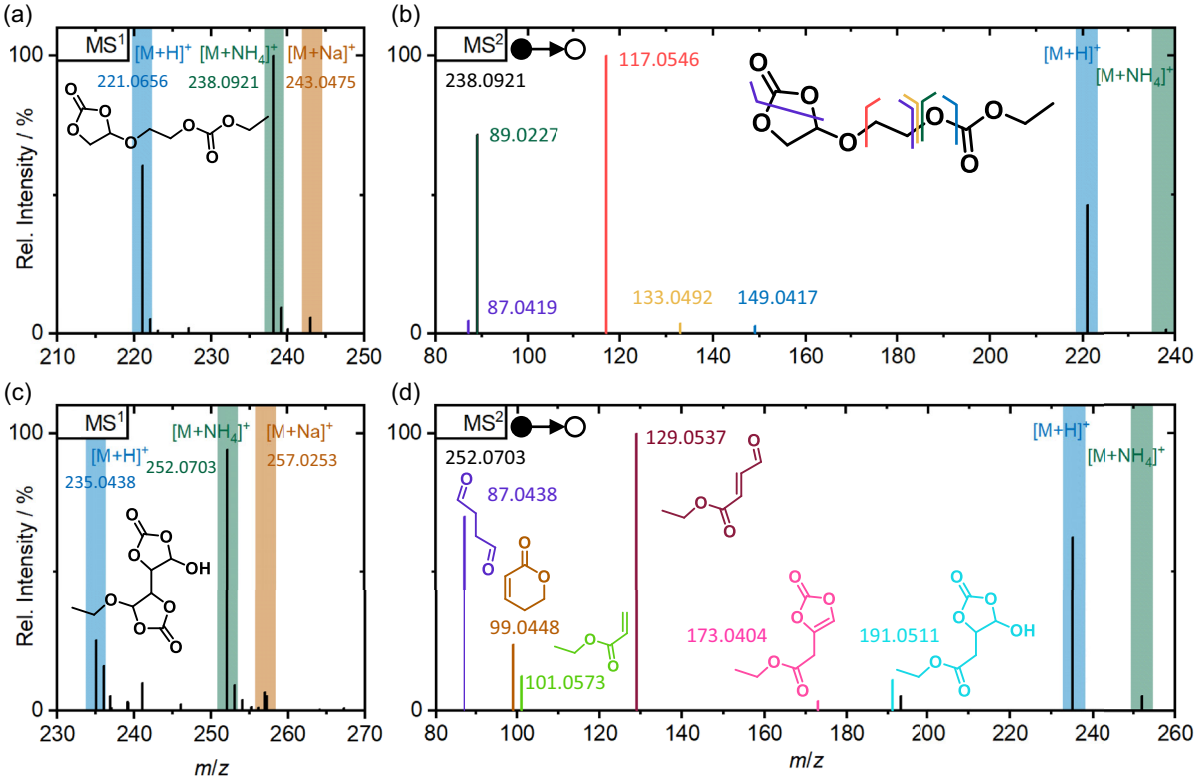

Figure 3. Mass spectra of different MS^1 and MS^2 experiments conducted for structure elucidation of FEC degradation product. The MS^1 spectra show different adducts for identification and MS^2 spectra fragments assigned to their respective formed structure and masses.

Figure 3a. In addition, degradation products with similar structures to the identified molecule were found with on ends containing VC reaction products (Figure 3c), which were shown in literature. Jin et al. postulated the generation of VC and polyVC for FEC electrolytes with glycol bond to one VC starting the polymerization reaction.[27] Degradation product *m/z* 252.0703 $[M+NH_4]^+$ consists of two VC units and terminal hydroxy end groups (Figure 3c). Structure validation was also performed by MS^2 fragmentation. The most intense fragment *m/z* 129.0537 $[M+H]^+$ corresponds to $C_6H_8O_3$ with DBE of 3 indicating the presence of VC as decarboxylation occurred for both VC units. Furthermore, fragment *m/z* 191.0511 $[M+H]^+$, which corresponds to $C_7H_{10}O_6$, supports the terminal OH group as well as two VC units. All additional fragments found support both structural proposals.

Different structures originating from FEC were identified containing different subgroups such as carbonate, glycol, or terminal OH. Most predominant degradation products show an oxygen linkage to the VC units which is displayed in HPLC-QToF chromatogram (**Figure 4**) for two structural analogs. In Figure 4, intensities for different terminal units and their retention time are shown. The retention in reversed phase (RP)-HPLC is based on van-der-Waals interaction between the analyte and the stationary phase. As previously shown by Henschel et al. longer terminal groups like ethyl compared to methyl increase the interaction and thereby retention of analytes.[36] Similar effects are observable for polyVC molecules. The molecule with oxygen linkage (Figure 4a) has the highest intensity for ethyl/hydrogen end group which was previously identified via MS^2. In contrast, terminal methyl or ethyl at the VC unit is less likely to form which is supported by observed intensities of terminal Me/Et and Et/Et groups for both molecules. The intensity of molecules for HPLC-MS measurements depend on the ionization conditions and by that also on the structure. Since the molecules exhibit similar structures, it can be assumed that their ionization behavior is comparable, allowing for direct comparison of intensities. In total, intensities for degradation products with no oxygen linkage to VC unit are decreased (Figure 4b). Furthermore, certain ethyl linkages suggest formation of these molecules via radical polymerization and unfavorable compared to ionic polymerization due to lower intensities. Again, structural similarities allow the direct comparison of intensities.

Further compounds with $(VC)_n$ have been identified by means of HPLC-QToF measurements. Molecules consist of different co-oligomers containing polyVC, glycol, or carbonates units. Notably, up to four polyVC, three carbonates, and one glycol unit bound to polyVC were detected. In total, 33 distinct degradation products and their respective isomers were found. Despite identification of these degradation products, it is suspected that higher varieties and chain lengths are generated. Liquid chromatographic techniques are limited to only detecting compounds that are soluble in the electrolyte, and by that not the composition of the SEI. As the chain lengths continues to increase, the polymeric species precipitate and get incorporated into the SEI. Furthermore, while Kubot et al. demonstrated the presence of PolyVC products in high voltage VC-containing electrolytes, the formation of the described degradation products in FEC electrolytes have not been confirmed by HPLC-QToF measurements yet.[38] The presence of characteristic terminal groups (ethyl/methyl) indicate the termination of degradation reaction products of EMC.[51]

3.2. Influence of FEC Concentration on Degradation

Degradation plays an important role in understanding aging of cells as it directly correlates to SEI composition. Thus, HPLC-QToF measurements enable conclusions regarding SEI formation and composition.[51,52] Varying FEC concentrations directly correlate to different amounts of degradation products, shown in **Figure 5**. Degradation products containing both polyVC and carbonates (a), as well as those containing polyVC (b), exhibit the highest intensity for F1, with decreasing intensities for F1.5 and F2. In contrast, only low intensities are detected for F3, and no signals are observed for STD. For higher cut-off voltages, intensities are increased compared to lower cut-off voltages but with same behavior in intensity (F1 > F1.5 > F2). Highest intensity is measured of oligo-fluoro-phosphates (OFP) (c) for FEC and EC containing electrolytes whereas lower intensity is obtained for STD or F3. Degradation products found containing polyVC incorporated in OFPs show the highest intensity for F3 decreasing for reduced FEC content, contrary to the previously observed trend.

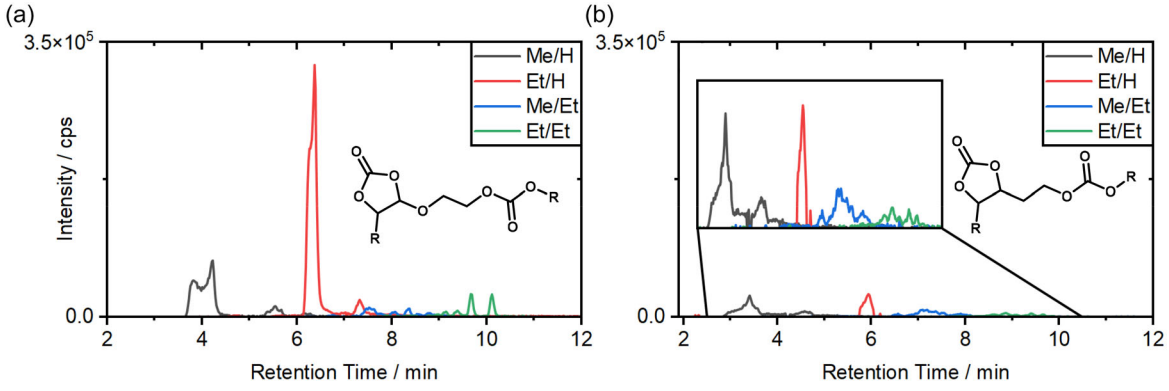

Figure 4. HPLC-QToF chromatograms of two degradation product analogs a) shows oxygen linkage to the VC unit, whereas b) not originating from FEC degradation. Intensities and retention time of different end groups (Me/H, Et/H, Me/Et, and Et/Et) are displayed.

Research Article
doi.org/10.1002/batt.202500610
Chemistry Europe
European Chemical Societies Publishing

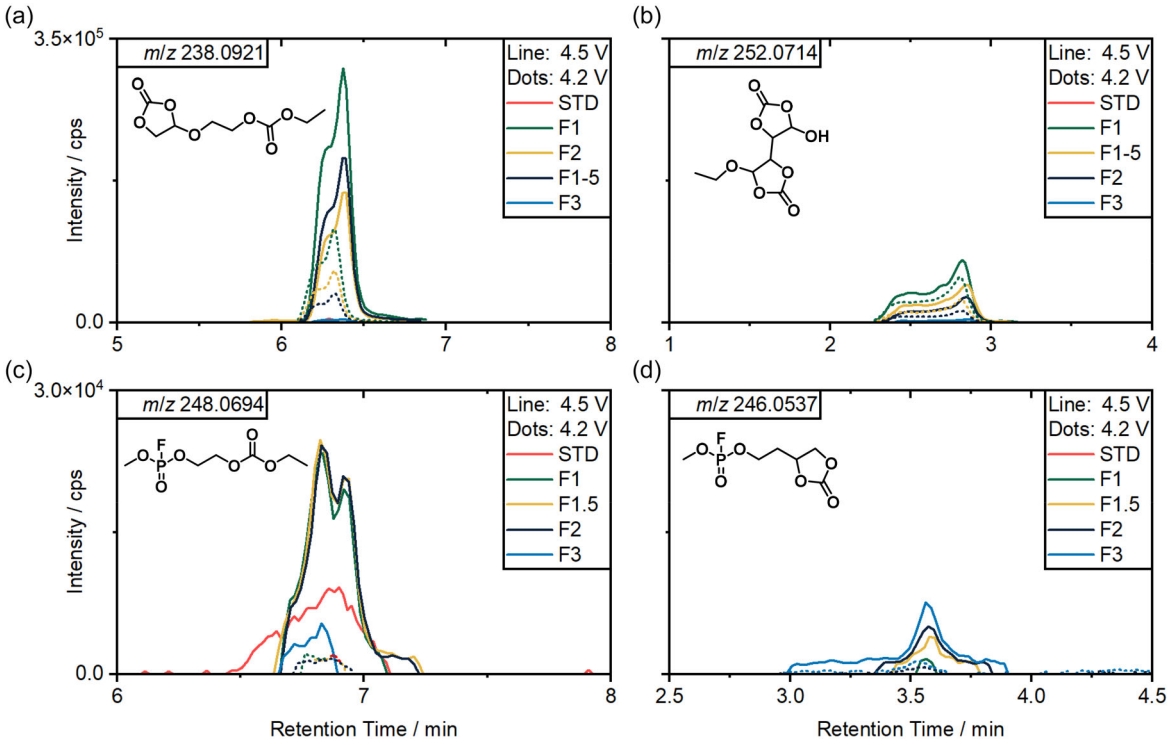

Figure 5. HPLC-QToF chromatograms of degradation products and their respective intensities for different FEC concentrations and different cut-off voltages (line: 4.5 V, point: 4.2 V). FEC degradation products containing polyVC and a) carbonates or b) polyVC are depicted. In addition, one c) OFP and d) OFP incorporated in polyVC are shown.

Thus, FEC could show the ability to scavenge OFPs but need further validation. Peak broadening in Figure 5b and d is observed which matches the high polarity of polyVC molecules and its weak interaction with nonpolar stationary phases. High voltage application can lead not only to increased amounts of degradation products but also different species due to additional oxidative degradation on the cathode side.[53] Hence, high voltage application of FEC electrolytes compared to STD, no difference in aspect of degradation species can be found. Nevertheless, the lower intensities observed for FEC-containing degradation products enable a general correlation with improved state of health of the electrolyte. Therefore, increased upper cut-off voltage only result in increased electrolyte consumption due to parasitic side reactions.

Decreased amounts of polyVC degradation products (Figure 5 a,b) for higher amounts of FEC can be correlated with electrochemical data. For high voltage applications, the electrochemical performance is worse for F1, as more side reactions with EC are possible. Therefore, long-term stabilization is likely caused by aging of the FEC electrolyte, which results in continuous formation of new SEI components. Moreover, higher OFP concentrations tend to attenuate the rollover effect, which contrasts with measured amounts of formed OFPs (Figure 5c). The reaction of OFP with in situ VC is most frequent with F3, as no competitive reaction with EC are possible. Thus, it is consistent with the assumption that polyVC aging products worsen the electrochemical performance as F3 shows the best long-term stability. The SEI would thicken during long-term cycling as more electrolyte degradation products, with high amounts of polyVC, would be incorporated into it. The thick SEI would increase the internal resistance and would hinder ion transport resulting in deteriorated battery performance.[54] The employment of EC-free electrolytes result in higher concentrations of OFP, improving cycling with higher cut-off voltages.[49] Similar behavior is seen here for F3 as the OFPs tend to react with VC forming polyVC containing OFPs.

The reaction of FEC and EC as cosolvents would result in decreased amounts of both electrolyte components. GC-flame ionization detector (FID) measurements after 600 cycles are displayed in **Figure 6**. For both upper cut-off voltages and STD (4.5 V: a), 4.2 V: b)), the transesterification products of EMC, dimethyl carbonate (DMC), and diethyl carbonate (DEC) are detected, which according literature, is a result of the formation of lithium alkoxides or lithium alkyl carbonates.[14,55–57] For all FEC electrolytes, no transesterification products can be found. This matches studies stating the use of film forming additive hindering or preventing the transesterification of EMC.[58–60] The ratio of EC in F1, F1.5, and F2 for both upper cut-off voltages show higher concentrations than in the initial electrolyte resulting in a decreased relation between FEC and EC. Thus, the assumption that FEC is consumed continuously and polymerizes is supported. Degradation products originating from EC immediately react with in situ formatted VC forming polyVC degradation products influencing the electrochemical performance as no VC was detected via GC-FID. In contrast, for F3, the FEC concentration decreases with increasing upper cut-off voltage, indicating that FEC is more likely to

Research Article
doi.org/10.1002/batt.202500610
Chemistry Europe
European Chemical Societies Publishing

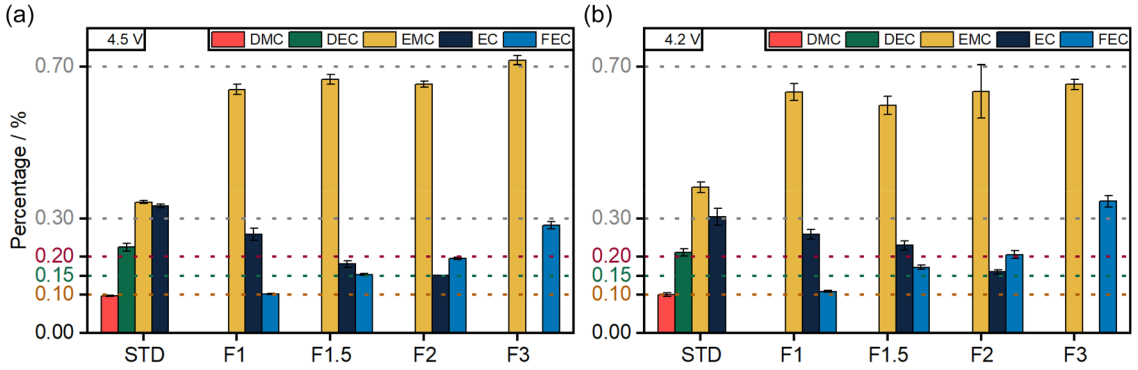

Figure 6. GC-FID measurements of the aged electrolyte after 600 cycles and upper cut-off voltage of a) 4.5 V and b) 4.2 V. Measured solvents were linear (DMC, DEC, and EMC) and cyclic carbonates (EC, FEC, and VC), which were in the initial electrolyte or possible formatted components. Percentages refer to ppm obtained from the measurement.

undergo reactions than EMC, which may contribute to improved long-term stability. The increased FEC concentrations for the lower cut-off voltage are more likely due to evaporated EMC during sample preparation.

In general, 33 different FEC degradation products have been found and identified. Whereas all follow the same intensity behavior shown in Figure 5, mostly, oxygen linkages between carbonate and polyVC backbone have been found, indicating degradation reactions to be primarily initiated by EC degradation products, which are consistent with FID measurements. In contrast, the EC-free electrolyte F3 shows nearly no FEC degradation products further supporting the assumption.

3.3. Degradation Mechanisms

The possible degradation mechanisms, which are shown in **Figure 7** of FEC, are postulated and already supported by different analytical studies.[25,61,62] Reaction 1, as described in the literature,

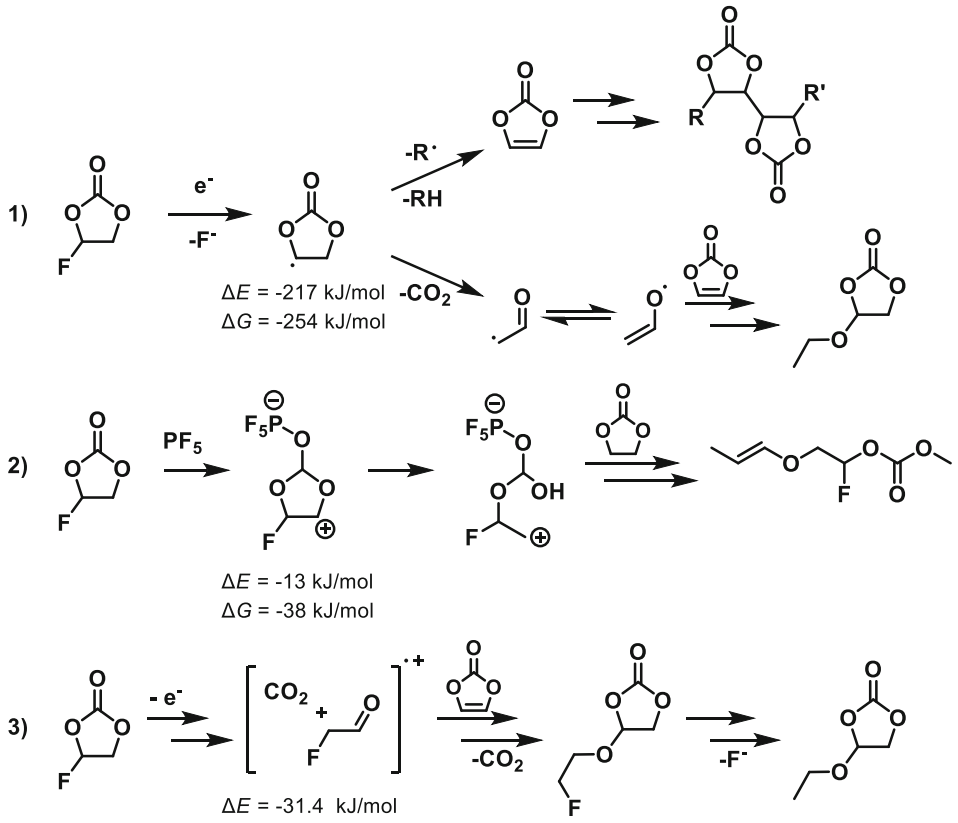

Figure 7. Different postulated reaction schemes for FEC degradation in LIB electrolytes. Reaction 1 is initiated by an cleavage of fluoride resulting in an EC radical, with subsequent reactions forming VC and ultimately VC degradation products.[27,64,65] Reaction 2 follows attachment of PF_5 on EC with following ring opening reaction resulting in fluorinated carbonate glycol co-oligomers.[25] Xia et al. calculated the energy release for the first reaction step of reaction 3.[66] Calculations were performed via DFT revealing reaction 1 to release more energy than reaction 2.

involves an initial electron transfer followed by F^- cleavage to form LiF. The exact mechanism and energetics, though, may vary between different reports. After additional hydrogen subtraction, in situ VC is formed which then further reacts with different VC molecules or other electrolyte components forming polyVC degradation products. The DFT calculations for the transition state of fluoride subtraction from FEC with the formation of an EC radical concluded an energy release of –217 kJ mol^{-1}. Additionally, the bond orders for FEC radical were calculated and revealed 0.71 for C—F bond and 0.63 for the carbonyl C—O bond. The lower binding energy order of the carbonyl C—O bond supports reaction 2. Reaction 2, published by Kim et al., follows the attachment of PF_5 on the carbonyl oxygen.[25] After ring opening reaction, PF_5 and CO_2 are released forming acetyl fluoride. DFT calculations revealed the released energy of –13 kJ mol^{-1} for the catalyzation via PF_5 on the carbonyl oxygen. Further calculations of subsequent reactions steps were not stable. The most predominant reaction occurring should follow reaction pathway 1 as more energy is released for the first transition state which then results in already found degradation products. Despite the lower bond order of the C—F bond compared to C—O bond, the greater energy release further supports reaction 1. Reaction 3 follows a decomposition route initiated by oxidative decomposition of FEC. Xia et al. postulated a ring-opening of FEC at the cathodic surface, resulting in CO_2 and 2-fluoroacetaldehyde radical cation with a released energy of -31.3 kJ mol^{-1}. As no other FEC-related degradation products were found, the radical can then react further with in situ formed VC to form the same degradation products of reaction 1. This agrees with the observed intensities of the degradation products, which are increased at an upper cut-off voltage of 4.5 V.

While it is not possible to prove that only one pathway is occurring during electrochemical operation, this study only found degradation products supporting reaction 1 and 3. Degradation products resulting from reaction 2 and its subsequent degradation pathways were not detected, suggesting it is not the predominant pathway. Additionally, the highest intensities of polyVC degradation products are found for the employment of EC and FEC. The reaction between both solvents is most likely to follow in situ formation of VC. As the most amounts of degradation products show an oxygen linkage the reaction is initiated by degradation of EMC or EC. Looking at the poor electrochemical performance for low FEC concentrations (F1) improving with higher FEC content, the degradation reactions should be initiated by EC decomposition products such as lithium ethylene dicarbonate (LEDC).[63] The oxygen linkage to the polyVC can be formed via ionic polymerization with an initiation by a nucleophilic attack on the VC or by the oxidative degradation product 2-fluoroacetaldehyde radical cation. Additionally, ethyl moieties can only occur via radical polymerization also originating from EC.[51] Therefore, the degradation reactions of VC can follow both ionic and radical polymerization forming the same degradation products.

4. Conclusion

In this study, electrolyte investigations after varying FEC and EC content in the electrolyte, including the replacement of EC by FEC, as well as the influence of different upper cut-off voltages (4.5 and 4.2 V), were performed. For both cut-off voltages, FEC/EMC showed the highest capacity and best capacity retention. Long-term experiments with higher cut-off voltages revealed that the use of FEC and EC as cosolvents (F1-F2) led to severe aging and poor electrochemical performance showing worse performance compared to STD. In contrast, for lower cut-off voltages, F1-F2 showed better long-term stability. Electrolyte investigations by means of HPLC-QToF were conducted investigating the influence of FEC as a cosolvent on electrolyte degradation. STD electrolyte showed the largest amount of degradation products, whereas for FEC-containing electrolytes, the total amount of degradation products decreased, not matching electrochemical data for high voltage applications. However, FEC related degradation products have been identified for the first time with instrumental analytical measurements. A long postulated degradation mechanism of FEC, which includes in situ formation of VC, has been approved. The VC then continues to react with EC or EMC in the electrolytes facilitating aging. Highest intensities in regard of FEC degradation products are found for F1 and decrease with increasing FEC content matching electrochemical data. Structural differences have been identified with an oxygen linkage between the polyVC backbone and terminal carbonate chains. Both structures can originate from EC or EMC degradation products initiating the polymerization of VC which can then follow both ionic as well as radical pathways. The upper cut-off voltages only showed influence on the amount of evolving degradation products but not the species itself indicating that ongoing FEC degradation results in worse electrochemical data. In total, 33 FEC related degradation products have been identified further supporting the postulation of in situ formed VC. This study illustrates the potential of FEC as replacement of EC for high voltage applications but simultaneously reveals the challenges when used as cosolvent.

Acknowledgements

The authors gratefully acknowledge funding support from LG Energy Solution. The authors sincerely thank Manuel Neumann for designing the graphical abstract.

Open Access funding enabled and organized by Projekt DEAL.

Conflict of Interest

The authors declare no conflict of interest.

Data Availability Statement

The data that support the findings of this study are available from the corresponding author upon reasonable request.

Keywords: analytical chemistry · electrolyte additive · electrolyte degradation · fluoroethylene carbonate · high voltage · lithium ion battery · reverse-engineering

[1] F. Degen, M. Winter, D. Bendig, J. Tübke, *Nat Energy* **2023**, *8*, 1284.
[2] Council of the European Union, can be found under, 6 June 2025) **2014**, https://www.consilium.europa.eu/de/policies/climate-change/2030-climate-and-energy-framework/(accessed.
[3] S. Jenu, I. Deviatkin, A. Hentunen, M. Myllysilta, S. Viik, M. Pihlatie, *J. Energy Storage* **2020**, *27*, 101023.
[4] J. T. Frith, M. J. Lacey, U. Ulissi, *Nat Commun* **2023**, *14*, 420.
[5] C. Liu, F. Li, L. Ma, H. Cheng, *Adv. Mater.* **2010**, *22*, E28.
[6] K. Xu, *Chem. Rev.* **2014**, *114*, 11503.
[7] M. Winter, R. J. Brodd, *Chem. Rev.* **2004**, *104*, 4245.
[8] IEA,, *International Energy Agency (IEA)* **2025**, Paris.
[9] K. Xu, *Chem. Rev.* **2004**, *104*, 4303.
[10] E. Peled, S. Menkin, *J. Electrochem. Soc.* **2017**, *164*, A1703.
[11] Y.-X. Lin, Z. Liu, K. Leung, L.-Q. Chen, P. Lu, Y. Qi, *J. Power Sources* **2016**, *309*, 221.
[12] J. Kim, O. B. Chae, B. L. Lucht, *J. Electrochem. Soc.* **2021**, *168*, 030521.
[13] J. S. Edge, S. O'Kane, R. Prosser, N. D. Kirkaldy, A. N. Patel, A. Hales, A. Ghosh, W. Ai, J. Chen, J. Yang, S. Li, M.-C. Pang, L. B. Diaz, A. Tomaszewska, M. W. Marzook, K. N. Radhakrishnan, H. Wang, Y. Patel, B. Wu, G. J. Offer, *Phys. Chem. Chem. Phys.* **2021**, *23*, 8200.
[14] C. Lechtenfeld, J. Buchmann, J. Hagemeister, M. M. Bela, S. Van Wickeren, S. Stock, R. Daub, S. Wiemers-Meyer, M. Winter, S. Nowak, *Advanced Science* **2024**, *11*, 2405897.
[15] X. Cheng, R. Zhang, C. Zhao, F. Wei, J. Zhang, Q. Zhang, *Advanced Science* **2016**, *3*, 1500213.
[16] I. Cekic-Laskovic, N. Von Aspern, L. Imholt, S. Kaymaksiz, K. Oldiges, B. R. Rad, M. Winter, in *Electrochemical Energy Storage*, R.-A. Eichel, Springer International Publishing, Cham **2019**, 1.
[17] S. H. Beheshti, M. Javanbakht, H. Omidvar, M. S. Hosen, A. Hubin, J. Van Mierlo, M. Berecibar, *IScience* **2022**, *25*, 103862.
[18] H. Adenusi, G. A. Chass, S. Passerini, K. V. Tian, G. Chen, *Adv. Energy Mater.* **2023**, *13*, 2203307.
[19] Y. S. Meng, V. Srinivasan, K. Xu, *Science* **2022**, *378*, eabq3750.
[20] M. Liu, J. Vatamanu, X. Chen, L. Xing, K. Xu, W. Li, *ACS Energy Lett.* **2021**, *6*, 2096.
[21] R. Lundström, N. Gogoi, T. Melin, E. J. Berg, *J. Phys. Chem. C.* **2024**, *128*, 8147.
[22] L. Hu, Z. Zhang, K. Amine, *Electrochem. Commun.* **2013**, *35*, 76.
[23] M. Leißing, C. Peschel, F. Horsthemke, S. Wiemers-Meyer, M. Winter, S. Nowak, *Batteries & Supercaps* **2021**, *4*, 1731.
[24] J. Liu, B. Li, J. Cao, X. Xing, G. Cui, *J. Energy Chem.* **2024**, *91*, 73.
[25] K. Kim, I. Park, S.-Y. Ha, Y. Kim, M.-H. Woo, M.-H. Jeong, W. C. Shin, M. Ue, S. Y. Hong, N.-S. Choi, *Electrochim. Acta* **2017**, *225*, 358.
[26] A. L. Michan, B. S. Parimalam, M. Leskes, R. N. Kerber, T. Yoon, C. P. Grey, B. L. Lucht, *Chem. Mater.* **2016**, *28*, 8149.
[27] Y. Jin, N.-J. H. Kneusels, P. C. M. M. Magusin, G. Kim, E. Castillo-Martínez, L. E. Marbella, R. N. Kerber, D. J. Howe, S. Paul, T. Liu, C. P. Grey, *J. Am. Chem. Soc.* **2017**, *139*, 14992.
[28] R. Pan, Z. Cui, M. Yi, Q. Xie, A. Manthiram, *Adv. Energy Mater.* **2022**, *12*, 2103806.
[29] J. S. Terreblanche, T. Luo, L. F. J. Piper, W. M. Dose, *Adv. Energy Mater.* **2025**, *15*, 2404427.
[30] T. Schwieters, M. Evertz, M. Mense, M. Winter, S. Nowak, *J. Power Sources* **2017**, *356*, 47.
[31] M. Evertz, C. Lürenbaum, B. Vortmann, M. Winter, S. Nowak, *Spectrochimica Acta Part B: Atomic Spectro.* **2015**, *112*, 34.
[32] W. Weber, V. Kraft, M. Grützke, R. Wagner, M. Winter, S. Nowak, *J. Chromatogr. A.* **2015**, *1394*, 128.
[33] S. Van Wickeren, L. Ihlbrock, C. Peschel, S. Wiemers-Meyer, M. Winter, S. Nowak, *J. Chromatogr. A.* **2025**, *1756*, 466070.
[34] C. Schultz, S. Vedder, B. Streipert, M. Winter, S. Nowak, *RSC Adv.* **2017**, *7*, 27853.
[35] J. Henschel, C. Peschel, F. Günter, G. Reinhart, M. Winter, S. Nowak, *Chem. Mater.* **2019**, *31*, 9977.
[36] J. Henschel, C. Peschel, S. Klein, F. Horsthemke, M. Winter, S. Nowak, *Angew Chem Int Ed* **2020**, *59*, 6128.
[37] J. Henschel, J. L. Schwarz, F. Glorius, M. Winter, S. Nowak, *Anal. Chem.* **2019**, *91*, 3980.
[38] M. Kubot, L. Balke, J. Scholz, S. Wiemers-Meyer, U. Karst, H. Hayen, H. Hur, M. Winter, J. Kasnatscheew, S. Nowak, *Adv. Sci.* **2024**, *11*, 2305282.
[39] J. Henschel, J. M. Dressler, M. Winter, S. Nowak, *Chem. Mater.* **2019**, *31*, 9970.
[40] R. Schmid, S. Heuckeroth, A. Korf, A. Smirnov, O. Myers, T. S. Dyrlund, R. Bushuiev, K. J. Murray, N. Hoffmann, M. Lu, A. Sarvepalli, Z. Zhang, M. Fleischauer, K. Dührkop, M. Wesner, S. J. Hoogstra, E. Rudt, O. Mokshyna, C. Brungs, K. Ponomarov, L. Mutabdžija, T. Damiani, C. J. Pudney, M. Earll, P. O. Helmer, T. R. Fallon, T. Schulze, A. Rivas-Ubach, A. Bilbao, H. Richter, et al., *Nat. Biotechnol.* **2023**, *41*, 447.
[41] M. J. Frisch, G. W. Trucks, H. B. Schlegel, G. E. Scuseria, M. A. Robb, J. R. Cheeseman, G. Scalmani, V. Barone, G. A. Petersson, H. Nakatsuji, X. Li, M. Caricato, A. V. Marenich, J. Bloino, B. G. Janesko, R. Gomperts, B. Mennucci, H. P. Hratchian, J. V. Ortiz, A. F. Izmaylov, J. L. Sonnenberg, F. Williams, F. Ding, F. Lipparini, F. Egidi, J. Goings, B. Peng, A. Petrone, T. Henderson, D. Ranasinghe, et al. **2016**.
[42] F. Pfeiffer, D. Diddens, M. Weiling, L. Frankenstein, S. Kühn, I. Cekic-Laskovic, M. Baghernejad, *Adv. Energy Mater.* **2023**, *13*, 2300827.
[43] M. Weiling, C. Lechtenfeld, F. Pfeiffer, L. Frankenstein, D. Diddens, J. Wang, S. Nowak, M. Baghernejad, *Adv. Energy Mater.* **2024**, *14*, 2303568.
[44] O. Borodin, M. Olguin, C. E. Spear, K. W. Leiter, J. Knap, *Nanotechnology* **2015**, *26*, 354003.
[45] A. V. Marenich, C. J. Cramer, D. G. Truhlar, *J. Phys. Chem. B.* **2009**, *113*, 6378.
[46] D. S. Hall, J. Self, J. R. Dahn, *J. Phys. Chem. C.* **2015**, *119*, 22322.
[47] T. Hou, K. D. Fong, J. Wang, K. A. Persson, *Chem. Sci.* **2022**, *13*, 8205.
[48] B. Flamme, G. R. Garcia, M. Weil, M. Haddad, P. Phansavath, V. Ratovelomanana-Vidal, A. Chagnes, *Green Chem.* **2017**, *19*, 1828.
[49] S. Klein, S. Van Wickeren, S. Röser, P. Bärmann, K. Borzutzki, B. Heidrich, M. Börner, M. Winter, T. Placke, J. Kasnatscheew, *Adv. Energy Mater.* **2021**, *11*, 2003738.
[50] S. Klein, P. Bärmann, T. Beuse, K. Borzutzki, J. E. Frerichs, J. Kasnatscheew, M. Winter, T. Placke, *ChemSusChem* **2021**, *14*, 595.
[51] C. Peschel, F. Horsthemke, M. Leißing, S. Wiemers-Meyer, J. Henschel, M. Winter, S. Nowak, *Batteries & Supercaps* **2020**, *3*, 1183.
[52] Y. P. Stenzel, F. Horsthemke, M. Winter, S. Nowak, *Separations* **2019**, *6*, 26.
[53] M. Kubot, B. Von Holtum, M. Winter, S. Wiemers-Meyer, S. Nowak, *J. Electrochem. Soc.* **2022**, *169*, 110534.
[54] L. Von Kolzenberg, A. Latz, B. Horstmann, *ChemSusChem* **2020**, *13*, 3901.
[55] H. Yoshida, T. Fukunaga, T. Hazama, M. Terasaki, M. Mizutani, M. Yamachi, *J. Power Sources* **1997**, *68*, 311.
[56] C. Schultz, V. Kraft, M. Pyschik, S. Weber, F. Schappacher, M. Winter, S. Nowak, *J. Electrochem. Soc.* **2015**, *162*, A629.
[57] N. Laszczynski, S. Solchenbach, H. A. Gasteiger, B. L. Lucht, *J. Electrochem. Soc.* **2019**, *166*, A1853.
[58] R. Petibon, L. Rotermund, K. J. Nelson, A. S. Gozdz, J. Xia, J. R. Dahn, *J. Electrochem. Soc.* **2014**, *161*, A1167.
[59] B. Strehle, S. Solchenbach, M. Metzger, K. U. Schwenke, H. A. Gasteiger, *J. Electrochem. Soc.* **2017**, *164*, A2513.
[60] F. Horsthemke, M. Leißing, V. Winkler, A. Friesen, L. Ibing, M. Winter, S. Nowak, *Electrochim. Acta* **2020**, *338*, 135894.
[61] Y. Ma, P. B. Balbuena, *J. Electrochem. Soc.* **2014**, *161*, E3097.
[62] R. Stockhausen, L. Gehrlein, T. Bergfeldt, A. Hofmann, F. J. Müller, J. Maibach, K. Hofmann, R. Gordon, A. Smith, *Batteries Supercaps* **2025**, *8*, e202400499.
[63] G. V. Zhuang, K. Xu, H. Yang, T. R. Jow, P. N. Ross, *J. Phys. Chem. B.* **2005**, *109*, 17567.
[64] N. V. Aspern, G.-V. Röschenthaler, M. Winter, I. Cekic-Laskovic, *Angew Chem. Int. Ed.* **2019**, *58*, 15978.
[65] I. A. Shkrob, J. F. Wishart, D. P. Abraham, *J. Phys. Chem. C.* **2015**, *119*, 14954.
[66] L. Xia, B. Tang, L. Yao, K. Wang, A. Cheris, Y. Pan, S. Lee, Y. Xia, G. Z. Chen, Z. Liu, *ChemistrySelect* **2017**, *2*, 7353.

Manuscript received: August 13, 2025
Revised manuscript received: October 20, 2025
Version of record online: